Dyes and Pigments 83 (2009) 155–161

Contents lists available at ScienceDirect

Dyes and Pigments

journal homepage: www.elsevier.com/locate/dyepig

The synthesis, characterization and electroluminescent properties of zinc(II) complexes for single-layer organic light-emitting diodes

He-Ping Zeng [a,*], Guang-Rong Wang [a], Gong-Chang Zeng [c], Jing Li [a,b,**]

[a] College of Chemistry, South China University of Technology, Guangzhou 510006, PR China
[b] Department of Chemistry and Chemical Biology, Rutgers University, 610 Taylor Road, Piscataway, NJ 08854, USA
[c] Department of Chemistry, McMaster University, 1280 Main St. W., Hamilton, ON L8S 4M1, Canada

ARTICLE INFO

Article history:
Received 4 January 2009
Received in revised form
3 March 2009
Accepted 4 March 2009
Available online 12 March 2009

Keywords:
Electroluminescence
Fluorescence spectra
Organic light-emitting diode (OLED)
8-Hydroxyquinoline derivative
Carbazole derivative
Zinc(II) complex

ABSTRACT

(E)-2-(2-(9-p-tolyl-9H-carbazol-3-yl)vinyl)-8-hydroxyl-quinoline, (E)-2-(2-(9-(4-methoxyphenyl)-9H-carbazol-3-yl)vinyl)-8-hydroxyquinoline and their respective zinc(II) complexes were synthesized and their structures confirmed using UV–vis, FT-IR, ESI-MS, FAB-MS, ^{1}H NMR and elemental analysis. The two Zn(II) complexes displayed high thermal stability with thermal decomposition temperatures of 422 °C and 410 °C, respectively. Photoluminescence spectra revealed that the complexes possessed maximum emissions at 575 and 570 nm, respectively, in the green region. Single-layer, organic light-emitting diodes built using these complexes emitted yellow light, as a result of a red-shift, with maximum luminances of 489 cd/m^2 and 402 cd/m^2 as well as luminance efficiencies of 0.41 cd A^{-1} and 1.81 cd A^{-1}, respectively.

1. Introduction

Organic light-emitting diodes (OLEDs) are making significant advances in flat panel display technology [1,2]. Some OLED products for car audio systems and mobile phone displays are in commercial volume production [3]. In a typical OLED, a hole transporter, an electron transporter, and a light emitter must be present. Carbazole derivatives are well known as hole-transporting and electroluminescent structure, because of their high charge mobility and photochemical stability, and because of their blue electroluminescence as a result of large band gap (improved planar biphenyl unit by the bridging nitrogen atom) [4,5]. In addition, the carbazole derivatives can be readily functionalized at 3-, 6-, or 9-position and covalently linked to other molecular units [6–10], resulting in a versatile synthesis of many types of derivatives. Substituting the hydrogen atom on nitrogen atom with alkyl chains, such as 2-ethylhexyl bromide and octylbromide, can increase the solubility of carbazole derivatives [4,11]. Therefore, the carbazole group has been commonly used as a functional building block in the fabrication of organic photoconductors, non-linear optical devices and OLEDs [12–15]. On the other hand, 8-hydroxyquinoline metal chelates are presently considered as one of the most reliable electro-transporting and emitting materials applied in molecular-based OLEDs for their thermal stability, high fluorescence, and excellent electron-transporting mobility [16–18]. In many cases, the electron-transporting mobility of zinc complexes with 8-hydroxyquinoline goes beyond that of aluminum complexes which is the most widely used electron-transporting material in OLEDs. Thus zinc complexes may be potential candidates to enhance the electron-transporting properties for OLEDs [12]. In recent years, it has been shown that a simple method to tune the emission wavelength and the efficiency of the devices is to modify the 2-, 5- or 7- position of the 8-hydroxyquinoline rings [19–22]. For optimal device performance, an equal rate of charge injection and charge transport is necessary at both electrodes. Low electroluminescence (LE) efficiency in some OLEDs is attributed mainly to an imbalance in the transportation rates of holes and electrons in the LE layer [23,24]. To balance the transport rates and improve the device performance of OLEDs, incorporating electron- and hole-transport units into the molecular structure of emitting materials is one of the commonly used strategy for chemical modification [25–31]. It is

* Corresponding author.
** Corresponding author. Institute of Functional Molecular, School of Chemistry and Chemical Engineering, South China University of Technology, Guangzhou 510641, China.
E-mail addresses: hpzeng@scut.edu.cn (H.-P. Zeng), jingli@rutgers.edu (J. Li).

0143-7208/$ – see front matter © 2009 Elsevier Ltd. All rights reserved.
doi:10.1016/j.dyepig.2009.03.003

conceivable that the overall cost will be reduced by a more simplified device fabrication. Thus it is desirable to design and synthesize compounds that combine the efficient hole-transport property of carbazole unit and the high electron-injection behavior of 8-hydroxyquinoline unit into a single material. On the basis of these considerations, we have succeeded in synthesizing two novel compounds bearing hole-facilitating carbazole units and electron-facilitating 8-hydroxyquinoline units and their respective zinc complexes (Scheme 1). Herein we report their synthesis, photoluminescent properties and performance as OLEDs.

2. Materials and instruments

2-Methyl-8-hydroxyquinoline, carbazole, 4-iodotoluene and 4-iodoanisole were purchased from Tokyo Kasei Kogyo Co. All chemicals were commercially available and were used without further purification, unless stated otherwise. Elemental analyses were carried out on a Finnigan analyzer. Mass spectra were recorded on a LCQ Advantage Max spectrometer. ^{1}H NMR spectra were taken on a Bruker DRX-400 MHz spectrometer with TMS as internal standard. UV–vis spectra were measured on a Cary 5000 spectrophotometer.

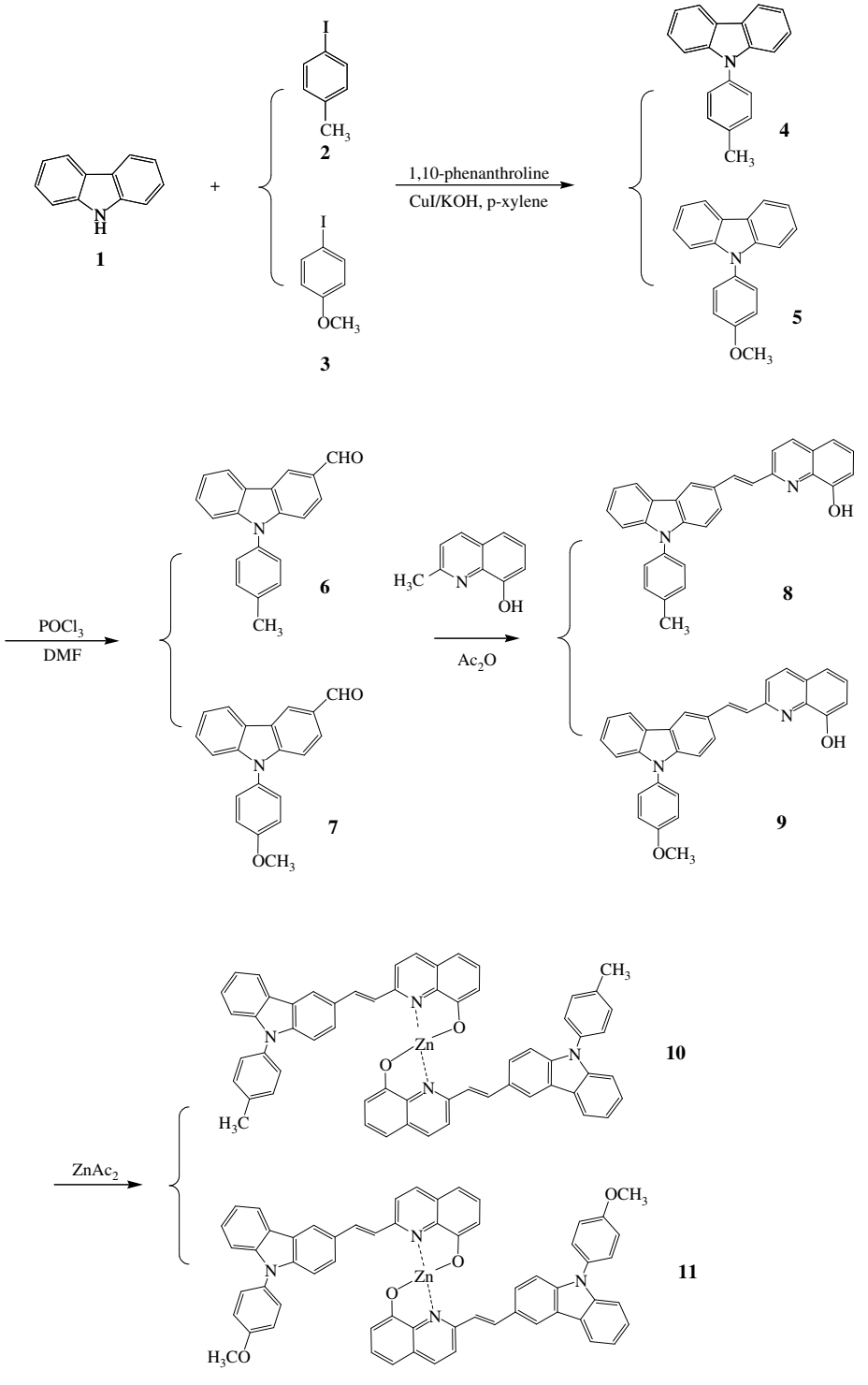

Scheme 1.

Fluorescence spectra and the fluorescence quantum yields were measured with a Fluorolog SpectroACQ fluorophotometer. IR experiments were conducted on a Perkin–Elmer 1730 and Tensor 27 FT-IR IR spectrometer. Melting points were determined using an XT-4 microscope melting point apparatus and were uncorrected. TG analysis was made on a thermal analyzer (TGA2050, TA Instruments, USA).

2.1. Synthesis of 9-p-tolyl-9H-carbazole (**4**) and 9-(4-methoxyphenyl)-9H-carbazole (**5**)

Compound **4** was synthesized according to the reported method [32] (Scheme 1). Carbazole **1** (6 mmol, 1.01 g), 4-iodotoluene **2** (6 mmol, 1.31 g), CuI (0.6 mmol, 0.12 g), 1,10-phenanthroline (0.6 mmol, 0.11 g) and potassium hydroxide powder (32.2 mmol, 2.35 g) were well mixed using a magnetic stirrer in 15 mL p-xylene under nitrogen atmosphere. The mixture was refluxed for 48 h. The products were neutralized by acetic acid and extracted with toluene. The toluene solution was concentrated under reduced pressure and yellowish powders were obtained. Suitable single colorless rod crystals of the product were obtained on slow solvent evaporation of petroleum ether (1.17 g, ca. 76% yield, m.p. 104 °C).

Colorless rod crystals of complex **5** were grown using the same reaction and corresponding procedure as that of complex **4** but employing **3** instead of **2**. (m.p. 155–156 °C, 1.26 g, 77% yield).

2.2. Synthesis of 9-p-tolyl-9H-carbazole-3-carbaldehyde (**6**) and 9-(4-methoxyphenyl)-9H-carbazole-3-carbaldhyde (**7**)

Compound **6** was synthesized from compound **4** according to the literature methods [32] (Scheme 1). The synthetic procedure is as follows.

Table 1
Crystallographic data for compounds **4** and **5**.

Compound	(**4**)	(**5**)
Molecular formula	$C_{19}H_{15}N$	$C_{19}H_{15}NO$
Molecular weight	257.32	285.33
Color and habit	Colorless rod	Colorless rod
Temperature (K)	298(2)	298(2)
Wavelength (nm)	0.071073	0.071073
Crystal system	Monoclinic	Monoclinic
Space group	*P*2(1)/*c*	*Pbca*
a (Å)	8.486(2)	8.3346(2)
b (Å)	21.053(6)	13.7502(3)
c (Å)	8.486(2)	13.7397(3)
α (°)	90	90.00
β (°)	107.38	107.241
γ (°)	90	90.00
V (Å^3)	1447.0(6)	1503.85(6)
Z	4	4
ρ (Mg m^{-3})	1.181	1.260
μ (mm^{-1})	0.068	0.078
F (000)	544	600
Crystal size (mm)	0.28 × 0.25 × 0.21	0.16 × 0.13 × 0.10
θ range for data collection (°)	2.51–25.24	2.15–25.24
h/*k*/*l* (max, min)	−10,10/−23,23/−10,10	−8,10/−16,16/−16,16
Reflections collected	11,600	8922
Independent reflections	2589 [*R*(int) = 0.0625]	2729 [*R*(int) = 0.0445]
Absorption correction	None	None
Refinement method	Full-matrix least-squares on F^2	Full-matrix least-squares on F^2
Data/restraints/parameters	2589/0/183	2729/2/400
Goodness-of-fit on F^2	1.174	1.025
Final *R*1[a], *wR*2[b] indices [$I > 2\sigma(I)$]	0.0560, 0.1763	0.0429, 0.1054
*R*1[a], *wR*2[b] indices (all data)	0.0790, 0.2151	0.0829, 0.1290
Largest difference peak and hole (e nm^{-3})	0.194 and −246	0.207 and −116

[a] $R = \sum(F_o - F_c)/\sum(F_o)$

[b] $Rw = [\sum w(F_o^2 - F_c^2)^2/\sum w(F_o^2)^2]^{1/2}$

Compound **4** (4.4 mmol, 1.14 g) was dissolved in a mixture of 10 mL DMF and 10 mL chlorobenzene. $POCl_3$ (26 mmol, 2.4 mL) was added dropwise into the mixture at room temperature. The mixture was stirred and heated to 85 °C for 24 h under nitrogen atmosphere. Upon cooling, the mixture was poured into an ice-bath and neutralized with sodium carbonate. The products were extracted with chloroform and purified by column chromatography on a silica gel column [4:1 petroleum ether:dichloromethane as eluent], giving a faint yellow solid product. Colorless, rod-shaped crystals of the product were obtained by evaporating the solvent from the product ethyl acetate saturated solution to afford **6** (m.p. 145–146 °C, 1.02 g, yield 81%).

Compound **7** was synthesized by similar process as that of compound **6** (yellow block crystals, m.p. 133–134 °C, 1.10 g, 82.5% yield).

2.3. Synthesis of (E)-2-(2-(9-p-tolyl-9H-carbazol-3-yl)vinyl)-8-hydroxyquinoline (**8**) and (E)-2-(2-(9-(4-methoxyphenyl)-9H-carbazol-3-yl)vinyl)-8-hydroxyquinoline (**9**)

The novel quinoline derivative **8** containing a carbazole unit was obtained by condensation between 2-methy-8-hydroxyquinoline and compound **6** (Scheme 1). The procedure to prepare ligand **8** is according to the reported method [29] and described as follows: A mixture of 2-methy-8-hydroxyquinoline (3.54 mmol, 0.56 g), **6** (3.54 mmol, 1.01 g) and acetic anhydride (15 mL) was stirred and heated at 130 °C for 48 h under nitrogen atmosphere. After being cooled, it was subsequently poured into 50 mL ice water and stirred for 3 h. The compound was extracted

Table 2
Crystallographic data for compounds **6** and **7**.

Compound	(**6**)	(**7**)
Molecular formula	$C_{20}H_{15}NO$	$C_{20}H_{15}NO_2$
Molecular weight	273.32	301.33
Color and habit	Colorless rod	Yellow block
Temperature (K)	298(2)	298(2)
Wavelength (nm)	0.071073	0.071073
Crystal system	Orthorhombic	Monoclinic
Space group	*Pn*	*P*2(1)/*n*
a (Å)	16.2650(8)	8.8891(2)
b (Å)	7.8175(4)	13.4861(3)
c (Å)	22.8040(10)	13.4779(4)
α (°)	90	90.00
β (°)	90	107.831
γ (°)	90	90.00
V (Å^3)	2899.6(2)	1538.11(7)
Z	8	4
ρ (Mg m^{-3})	1.252	1.301
μ (mm^{-1})	0.077	0.084
F (000)	1152	632
Crystal size (mm)	0.12 × 0.10 × 0.08	0.20 × 0.18 × 0.14
θ range for data collection (°)	1.79–27.55	2.19–27.58
h/*k*/*l* (max, min)	−21,20/−10,10/−29,29	−11,10/−17,13/−17,16
Reflections collected	33,321	7490
Independent reflections	3324 [*R*(int) = 0.0882]	3543 [*R*(int) = 0.0310]
Absorption correction	None	None
Refinement method	Full-matrix least-squares on F^2	Full-matrix least-squares on F^2
Data/restraints/parameters	3324/0/192	3543/0/210
Goodness-of-fit on F^2	0.990	1.034
Final *R*1[a], *wR*2[b] indices [$I > 2\sigma(I)$]	0.0521, 0.1241	0.0465, 0.1078
*R*1[a], *wR*2[b] indices (all data)	0.1317, 0.1557	0.0835, 0.1247
Largest difference peak and hole (e nm^{-3})	0.129 and −147	0.146 and −130

[a] $R = \sum(F_o - F_c)/\sum(F_o)$

[b] $Rw = [\sum w(F_o^2 - F_c^2)^2/\sum w(F_o^2)^2]^{1/2}$

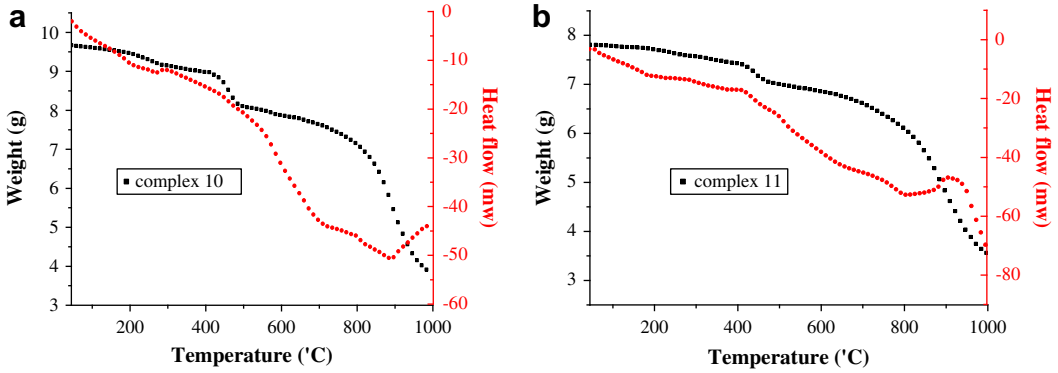

Fig. 1. (a) Thermal gravimetric analysis curves of complex **10**. (b) Thermal gravimetric analysis curves of complex **11**.

to yield yellow organic precipitate by dichloromethane. The solvent was then removed under reduced pressure and final product was purified by gel column chromatography using petroleum ether/ethyl acetate (10:1) as eluent, the product is a yellow solid, weighing 0.943 g, yielding 62.5%. m.p. 149–150 °C. UV (in DMF) λ_{max}: 379, 305 nm; FTIR (KBr) ν: 3389, 3029, 2954, 1645, 1593–1507, 1335 cm^{-1}; MS (ESI) m/z: 427 $(M+H)^+$, ^1H NMR ($CDCl_3$, 400 MHz) δ: 2.37 (s, 3H, CH_3), 7.04 (d, $J=7.6$ Hz, H, ArH), 7.10–7.16 (m, 2H, ArH), 7.20 (d, $J=8.0$ Hz, 2H, ArH), 7.24 (d, $J=7.4$ Hz, H, ArH), 7.26–7.34 (m, 2H, ArH), 7.41 (d, $J=16.0$ Hz, vinylic H) 7.44–7.48 (m, 2H, ArH), 7.51 (d, $J=7.8$ Hz, 2H, ArH), 7.54 (d, $J=8.2$ Hz, H, ArH), 7.56–7.61 (m, 2H, ArH), 7.72 (d, $J=16.0$ Hz, vinylic H), 7.87 (d, $J=8.0$ Hz, H, ArH), 9.18 (s, H, OH) analytically calculated for $C_{30}H_{22}N_2O$: C 84.48, H 5.20, N 6.57; found C 84.61, H 5.23, N 6.51.

Compound **9** was obtained by the same way as that of compound **8**, but using **7** instead of **6**. It is a yellow solid, weighing 0.958 g (61.2% yield), m.p. 147–148 °C. UV–vis (DMF) λ_{max}: 379, 305 nm; IR (KBr) ν: 3386, 3030, 2951, 1624, 1589–1510, 1334, 1240 cm^{-1}; MS (ESI) m/z: 443 $(M+H)^+$, ^1H NMR ($CDCl_3$, 400 MHz) δ: 3.82 (s, 3H, CH_3), 6.90 (d, $J=7.6$ Hz, 2H, ArH), 7.02 (d, $J=7.6$ Hz, H, ArH), 7.08–7.14 (m, 2H, ArH), 7.22 (d, $J=7.4$ Hz, H, ArH), 7.25–7.33 (m, 2H, ArH), 7.40 (d, $J=16.0$ Hz, vinylic H) 7.42–7.47 (m, 2H, ArH), 7.50 (d, $J=7.8$ Hz, 2H, ArH), 7.56 (d, $J=8.2$ Hz, H, ArH), 7.58–7.62 (m, 2H, ArH), 7.72 (d, $J=16.0$ Hz, vinylic H), 7.86 (d, $J=8.0$ Hz, H, ArH), 9.16 (s, H, OH) analytically calculated for $C_{30}H_{22}N_2O_2$: C 81.43, H 5.01, N 6.33; found C 81.52, H 5.04, N 6.27.

*2.4. Preparation of zinc(II) complex bis[2-(2-(9-p-tolyl-9H-carbazol-3-yl)vinyl)-8–hydroxyquinoline] zinc(II) (**10**) and bis[2-(2-(9-(4-methoxyphenyl)-9H-carbazol-3-yl)vinyl) -8-hydroxyquinoline]zinc(II) (**11**)*

Complex $Zn(C_{30}H_{21}N_2O)_2$ **10** was prepared from ligand **8** and zinc acetate dihydrate in DMF (Scheme 1) according to procedures described elsewhere [33].

Zinc acetate dihydrate (2.2 mmol, 0.413 g) was dissolved in 45 mL anhydrous methanol. The Zn(II) solution was added dropwise into the DMF (90 mL) solution of ligand **8** (2.2 mmol, 0.94 g), and kept stirring for 24 h. The yellow precipitate was filtered off, washed with methanol and dried in vacuum to afford **10**: 0.835 g, yield 72.8%. m.p. >300 °C; IR (KBr) ν: 3033, 2956, 1642, 1594–1513, 1337, 514, 488 cm^{-1}; FAB-MS m/z: 915 $(M+H)^+$, analytically calculated for $Zn(C_{30}H_{21}N_2O)_2$:, C 78.57, H 4.58, N 6.11; found C 78.73, H 4.60, N 6.08.

Complex $Zn(C_{30}H_{21}N_2O_2)_2$ **11** was obtained by the similar way as that of compound **11**, but using **9** instead of **8** (0.824 g, 68.9% yield, m.p. >300 °C); IR (KBr) ν: 3025, 2954, 1648, 1592–1514, 1336, 1244, 515, 485 cm^{-1}; FAB-MS m/z: 947 $(M+H)^+$, analytically calculated for $Zn(C_{30}H_{21}N_2O_2)_2$; C 75.92, H 4.43, N 5.90; found C 76.03, H 4.46, N 5.87.

2.5. X-ray crystallography

The crystals of compounds **4–7** were mounted onto thin glass fibers in air for X-ray measurement. Crystal structures were

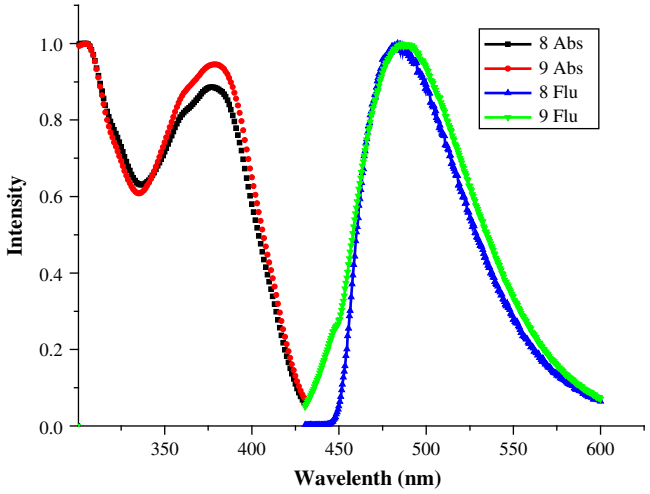

Fig. 2. Absorption and fluorescence spectra of complexes **8** and **9** in DMF.

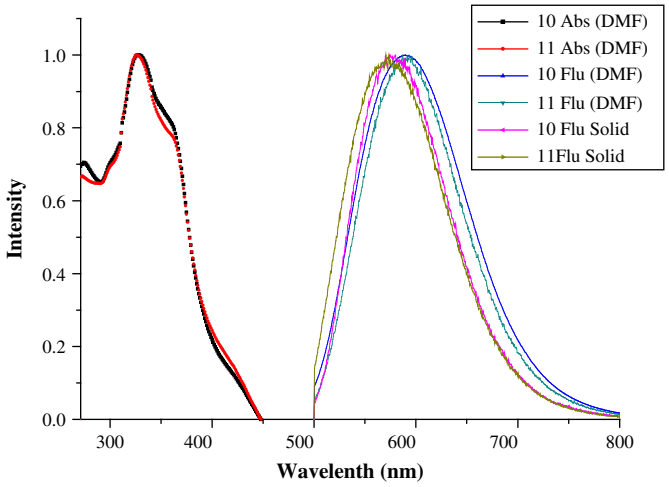

Fig. 3. Absorption and fluorescence spectra of complexes **10** and **11**.

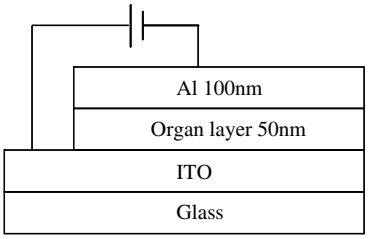

Fig. 4. Structure of the single-layer OLED.

determined from X-ray data collected on a Siemens (Bruker) SMART APEX II diffractometer with graphite-monochromated Mo Kα radiation ($\lambda = 0.71073$ Å) at room temperature using the program SMART and processed by SAINT (Bruker AXS Inc., Madison, WI, USA). Absorption corrections were applied using SADABS (Sheldrick, 1996). The structures were solved by direct methods using SHELXS97 (Sheldrick, 1997) and refined by least-squares on F2 using SHELXTL/PC (Bruker AXS Inc.).

Compounds **4**–**7** crystallize in the space groups of *P*2(1)*c*, *Pbca*, *Pn* and *P*2(1)/*n*, respectively. Anisotropic displacement parameters were applied for the ordered non-H atoms in the structures. H-atom positions were calculated by geometrical methods and refined using a riding model. Crystallographic data and experimental details for structure analyses are summarized in Tables 1 and 2.

2.6. Thermal properties of complexes *10* and *11*

The thermal properties of complexes **10** and **11** were investigated by thermogravimetric analysis. The samples were heated in the range of 45–1100 °C at a heating rate of 10 °C/min and at a nitrogen gas rate of 80 mL/min on a thermal analyzer (TGA2050, TA Instruments, USA). Under these conditions, no clear melting temperature (T_m) was observed, indicative of their amorphous character. Complexes **10** and **11** lost weight gradually during the early phase of the experiment. TGA shows (Fig. 1) that **10** and **11** lost about 2.0% weight from 45 to 422 °C and 410 °C, respectively, the weight loss is possibly due to volatilization. Then the samples underwent an accelerated weight loss, 9.12% weight loss of **10** from 422 to 500 °C, with an onset decomposition temperature (*T*d) at ~422 °C, while **11** lost 12.4% from 410 to 485 °C. The weight loss is in agreement with the calculated amount of two CH_3 and two C_2H_2 in **10**, and two OCH_3 and two C_2H_2 in **11**. There were hardly weight loss in the third phase with **10** from 500 to 560 °C, **11** from 485 to 585 °C, and in the last temperature range, a significant amount of weight loss was observed in both cases, indicating a nearly complete decomposition. The thermal analysis results indicate that complexes **10** and **11** have high T_d and good thermal stability, which is very desirable for fabricating stable organic EL devices.

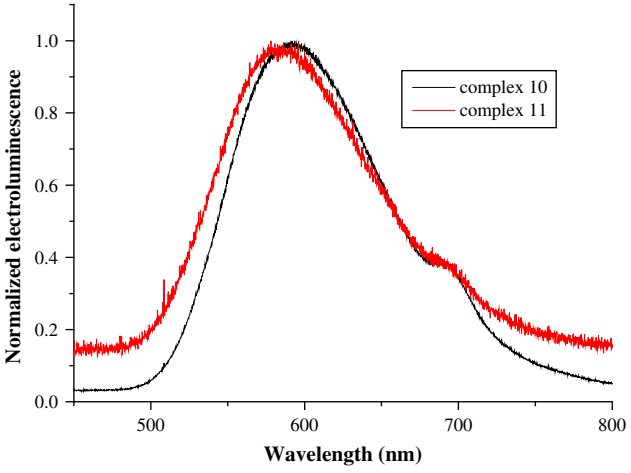

Fig. 5. The electroluminescence spectrum of complexes **10** and **11**.

2.7. Optical absorption and photoluminescent spectra

The photophysical properties including absorption and fluorescent characteristics of **8**–**11** have been studied. Fig. 2 shows the room-temperature absorption and fluorescent spectra of **8** and **9** in the DMF; the solution of **8** and **9** exhibits an absorption maximum at 305 nm to the accompaniment of a shoulder peak at 376 nm. The absorption bands in the 250–380 nm range can be assigned to intraligand (π–π^*) transitions. Upon irradiation by UV-light at room temperature, the **8** and **9** solution shows a blue emission with a peak at 487 nm.

The photoluminescent (PL) spectra of ligands **8** and **9**, in all solvents used, were recorded with an excitation wavelength $\lambda_{ex} = 420$ nm. It indicates that the relative intensity of the PL does not change in different solvent, which shows the intensity of the PL isn't in relation with solvent polarity. Ligands **8** and **9** give a maximum emission peak centered ranged from 468 to 486 nm individually. These suggest that ligands **8** and **9** in all solvents emit blue-green light with ligand **8** in DMF, THF, toluene with corresponding maximum emission at 484, 471 and 468 nm, while ligand **9** with corresponding maximum peak located at 486, 473 and 469 nm. The results show that PL peaks were slightly red-shifted from 468 nm to 484 nm for ligand **8** and from 469 nm to 486 nm for ligand **9**, respectively with the increase in solvent polarity. It is proved that the Stokes shift is in direct proportion with the solvent polarity [30]. It is believed that the scale of solvent polarizability parameter, which measures the ability of the medium to stabilize the charge on a dipole by virtue of its dielectric effects [33].

Fig. 3 shows the room-temperature absorption and fluorescent spectra of **10** and **11** in the solution and thin film. The solution of **10** and **11** exhibits an absorption maximum at 326 nm to the accompaniment of a shoulder peak at 355 nm. It also can be assigned to intraligand (π–π^*) transitions. Upon irradiation by UV-light at room temperature, the **10** and **11** solution shows a green emission with a peak at 547 nm; and solid emission with a peak at 591 nm, the ligand exhibits a blue one at 487 nm. Therefore, we suggest that coordination of the ligand with the zinc ion results in the usual red-shift observed for most of the complexes.

The fluorescent spectra of the metal zinc complexes were measured in DMF solution and solid states at room temperature, shown in Fig. 3. Their maximum emission is extraordinarily red-shifted in comparison with bis(2-methy-8-hydroxy)zinc(II) ($\lambda^{em}{}_{max} = 515$ nm), it has been argued their luminescent performance is changed by modify the 2-position of the 8-hydroxyquinoline rings [22]. The peaks of the PL spectra of these two complexes in DMF solution and solid states were at around 547 and 591 nm when excited at 468 nm, respectively, giving off green light, and as expected, the introduction of zinc(II) to ligands **9** and **10** leading to a red-shift compared to their respective ligands (483 nm and 487 nm). The difference in emission spectra indicates that the metal zinc(II) affects substantially emission spectra of the compounds. The emission spectra in solid state show significant similitude to that in the DMF solution. The solid complexes **10** and **11** gave a maximum emission peak occurred at 575 nm, 591 nm individually when excited at 468 nm, giving off green light, and

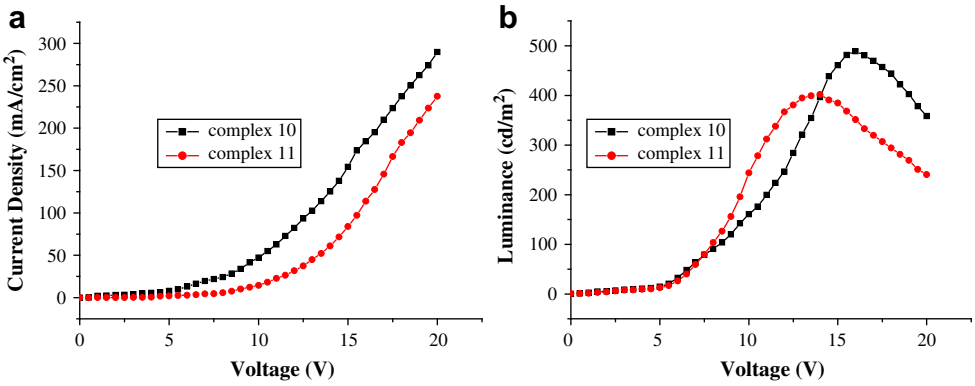

Fig. 6. (a) Current density–voltage curves (*J*–*V*) characteristics for the OLEDs. (b) Luminance–voltage (*L*–*V*) characteristics for the OLEDs.

showed a blue-shift ca 20 nm in comparison with their each DMF solution, and this can be attributed to the difference in the torsional angles between carbazole–phenyl units in solution and the twisted structure in the solid state [34]. This phenomenon is also observed in analogous polymers in the polymer backbone [35].

2.8. EL device fabrication and EL characteristic

The electroluminescence performance of these complexes was examined using a single-layer device configuration. The OLED devices containing zinc complexes **10** or **11** were fabricated by vacuum deposition. A commercial indium tin oxide (ITO)-coated glass was acted as the substrate, The ITO-coated glass was pretreated according to a regular chemical cleaning using detergent, deionized water and alcohol in sequence, followed by ozone cleaning, used as an anode. The thermal evaporation of organic materials was carried out at a chamber pressure of 10^{-6} Torr. The complexes **10** or **11** were deposited in 50 nm thick layers with, respectively, at a rate 1–2 Å/s, followed by a 100 nm thick layer of Al used as the cathode. The OLEDs were not encapsulated. The schematic diagram of the EL devices is shown in Fig. 4.

The current–voltage (*I*–*V*) curve and the luminescence–voltage (*L*–*V*) curve were obtained using Fluorolog-3 instruments (Instruments, S.A. Inc.). The measurements were carried out at ambient conditions.

The EL spectra of the OLEDs are shown in Fig. 5 while their current density–voltage (*J*–*V*) and luminance density (*L*–*J*) characteristics are shown in Fig. 6. The OLED devices with compounds **10** and **11** all showed yellow electroluminescence (EL) with broad EL spectra ranging from 500 to 750 nm, showing some red-shifts relative to photoluminescence (PL) spectra in solid state. It may be that intermolecular processes and excited formation between adjacent chromophore are greatly strengthened in compact organic layer of the OLEDs, leading to a red-shift of the emission spectra.

Fig. 6(a) and (b) shows the luminance and current density versus the applied voltage of the device. The forward bias current was obtained when the ITO was a positive electrode and the Al a negative one. The current and light output increased with increase in the forward bias voltage and the turn-on voltage of the devices was all about 5 V. The devices exhibit good stability, when they work at the operating voltage. The maximum luminance of the device based on **10** that could be achieved was about 489 cd/m^2 when the voltage reached 16 V, which corresponding to current density is 185 mA/cm^2, and luminance efficiency 0.41 cd/A. Whereas the corresponding performance of the device based on **11** are 402 cd/m^2, 14 V, and 61 mA/cm^2, 1.81 cd/A, respectively. From the results, we can see that complex **10** is superior to complex **11** at luminance performance in fabricating single-layer OLED, but complex **11** does much better in luminance efficiency. However the difference of the performance between **10** and **11** still cannot be well explained. Detailed electroluminesent studies of these complexes and further research on optimum conditions for the OLED fabrication are underway in our laboratory.

3. Conclusion

We have synthesized two new ligands containing electron-transporting 8-hydroxyquinoline units and hole-transporting carbazole units and their respective zinc(II) complexes. The spectroscopic studies have been carried out on all four compounds and our findings clearly demonstrate that fine control of the photophysical properties is possible through the modification of substitute in position 2 of the 8-hydroxyquinoline rings. The two zinc(II) complexes have high thermal stabilities and the thermal decomposition temperatures are 390 °C and 415 °C. Two single-layer EL device based on **10** and **11** has been demonstrated by the conventional vacuum evaporation method, and the voltage-induced evolution of the EL spectra of the device has been observed. The low luminance would be due to the thickness of organic emitting layer in the OLEDS and optimization of the fabrication procedure will improve it. The phenomena are attributed to further research on optimum conditions for the OLED, the fabrication of different constitution is in progress in our laboratory, making them useful for practical application in organic light-emitting devices.

Acknowledgement

Financial support from the National Natural Science Foundation of China (Nos.: 20671036, 2006A10801002, 2007A010500008 and 2008B010800030) is gratefully acknowledged. JL is a Cheung Kong Scholar associated with SCUT.

References

[1] Hogan H. Photon Spectra 2003;37:66.
[2] Xiao HB, Shen H, Lin Y, Su JH, Tian H. Dyes Pigments 2007;73:224.
[3] Bardsley JN, Sel IJ. Top Quantum Electron 2004;10:3.
[4] Morin JF, Leclerc M. Macromolecules 2002;35:8413.
[5] Brunner K, Dijken AV, Börner H, Bastiaansen JAM, Kiggen NMM, Langeveld BMW. J Am Chem Soc. 2004;126:6035.
[6] Wang YZ, Epstein AJ. Acc Chem Res 1999;32:217.
[7] Maaruyama S, Tao X-T, Hokari H, Noh T, Zhang Y, Wada T, et al. J Mater Chem 1999;9:893.
[8] Zhu Z, Moore Js. J Org Chem 2000;65:116.
[9] Xie JT, Ning ZJ, Tian H. Tetrahedron Lett 2005;46:8559.
[10] Xu ZW, Li Y, Ma XM, Gao XD, Tian H. Tetrahedron 2008;64:1860.

[11] Jung H-K, Lee CL, Lee JK, Kim JK, Park SY, Kim JJ. Thin Solid Films 2001;401:111.
[12] Hamada Y, Sano T, Fujita M, Fujii T, Nishio Y, Shibata K. Jpn J Appl Phys 1993;32:L514.
[13] Fitilis I, Fakis M, Polyzos I, Giannetas V, Persephonis P, Vellis P, Mikroyannidis J. Chem Phys Lett 2007;447:300.
[14] Sienkowska MJ, Monobe H, Aszynski PK, Shimizu Y. J Mater Chem 2007;17:1392.
[15] Lee SJ, Park JS, Yoon K-J, Kim Y-I, Jin S-H, Kang SK. Adv Funct Mater 2008;18:3922.
[16] Brinkmann M, Fite B, Pratontep S, Chaumont C. Chem Mater 2004;16:4627.
[17] Khalifa MB, Vaufrey D, Tardy J. Org Electron 2004;5:187.
[18] Mirzaee M, Amini MM. Appl Organomet Chem 2005;19:339.
[19] Ghedini M, Deda ML, Aiello I, Grisolia A. Inorg Chim Acta 2004;357:33.
[20] Pohl R, Montes VA, Shinar J, Anzenbacher P. J Org Chem 2004;69:1723.
[21] Barberis VP, Mikroyannidis JA. Synth Met 2006;156:865.
[22] Sharma A, Singh D, Makrandi JK, Kamalasanan MN, Shrivastva R, Singh I. Mater Lett 2007;10:1016.
[23] Ahn T, Shim HK. Macromol Chem Phys 2001;202:3180.
[24] Zheng M, Ding L, Gurel EE, Karasz FE. J Polym Sci Part A Polym Chem 2002;40:235.
[25] Huang Q, Cui J, Yan H, Veinot JGC, Marks TJ. Appl Phys Lett 2002;81:3528.
[26] Kim JJ, Kim KS, Baek S, Kim HC, Ree M. J Polym Sci Part A Polym Chem 2002;40:1173.
[27] Li ZH, Wong MS, Fukutani H, Tao Y. Org Lett 2006;8:4271.
[28] Huang TH, Lin JT, Chen LY, Lin YT, Wu CC. Adv Mater 2006;18:602.
[29] Lane PA, Kushto GP, Kafafi ZH. Appl Phys Lett 2007;90:023511.
[30] Tse SC, Tsung KK, So SK. Appl Phys Lett 2007;90:213502.
[31] Aubouya L, Gerbier P, Gúerin C, Hirsch L, Vignau L. Synth Met 2007;157:91.
[32] Lee TH, Tong KL, So SK, Leung LM. Synth Met 2005;155:116.
[33] Jing H-L, Zeng H-P, Zhou Y-D, Wang T-T, Yuan G-Z, Ouyang X-H. Chin J Chem 2006;24:966.
[34] Jung S-H, Kim D-Y, Cho H-N, Suh D-H. J Polym Sci Part A Polym Chem 2006;44:1189.
[35] Jung SH, Suh DH, Cho HN. Polym Bull (Berlin) 2003;50:51.